SUM-RULES, STRENGTH DISTRIBUTIONS AND GIANT RESONANCES[+]

O. BOHIGAS

Division de Physique Théorique[*], Institut de Physique Nucléaire
F-91406 ORSAY CEDEX

IPNO-TH 80-13 March 1980

---

[*]Laboratoire associé au C.N.R.S.

[+]Invited talk delivered at the International Conference on "Theory and applications of moment methods in many fermion systems" September 1979, Ames, Iowa

1. Introduction

It is well known that atomic nuclei show collective properties. One important aspect of collective motion is the concentration in energy of excitation strength. This is best illustrated by the nuclear photo effect [1] which has the following two main characteristics : i) the photoabsorption cross-section shows, all over the periodic table, a broad peak that takes a large part of the integrated photo cross-section, ii) the variation of the peak energy is a smooth function of the mass number A. Two main routes can be followed in order to describe such a behaviour

1) the more detailed, in which the strength function $S(E)$ is calculated at all energies E
2) a more global in which only some energy moments of the strength function $S(E)$ are computed

The purpose of this talk is to describe some methods and applications corresponding mainly to the second route. A description of the strength distribution by its energy moments or sum-rules will be especially suited when the excitation strength is highly collective, in which case one can hope that the knowledge of a very limited number of moments will give the salient features of $S(E)$. Would $S(E)$ have a complicated structure as a function of E then many moments would be required in order to reproduce its properties (see contributions of P. Langhoff and J.C. Wheeler to this conference).

The kind of questions we shall address ourselves when dealing with sum-rules are : do they have a clear physical meaning, can they be extracted directly from experimental data

are they model dependent, to which kind of correlations are they sensitive to, which properties of effective interactions do they reflect, can they be computed easily ? Let us anticipate by saying that some particular sum-rules, besides being a means to reconstruct the strength function, have indeed a direct physical meaning and are therefore interesting by themselves.

The material of this talk is organized as follows : In section 2 we give some general properties of sum-rules. In section 3 we discuss the experimental situation concerning the photoabsorption cross-sections (E1, T = 1 mode) and the electric isoscalar monopole (E0, T = 0 mode) and quadrupole (E2, T = 0 mode) giant resonances. In section 4 we discuss the corresponding theoretical sum-rule approaches, with special emphasis on selfconsistent methods, and we end up with some general conclusions.

Various aspects of sum-rule techniques can be found in reviews, textbooks or lecture notes [1-5] . In this talk several important questions of current interest in this field will not be touched. Let us particularly mention the problem of location and interpretation of magnetic dipole strength in nuclei [6,7], the discussion of electronuclear sum-rules [8-10] and the role of sum-rules in relating different versions of collective theories [34-36].

2. General properties of the strength function [11]

When a system with hamiltonian $H = T + V$ is perturbed by an external oscillating field $Q\cos(Et/\hbar)$ the response can be expressed by the time averaged expectation value of the perturbing operator and is given by the dynamic polarizability $\alpha(E)$

$$\alpha(E) = \langle 0|Q\, G(E) Q|0\rangle \tag{2.1}$$

where $G(E)$ is the Green function

$$G(E) \equiv (H-\mathcal{E}_0-E)^{-1} + (H-\mathcal{E}_0+E)^{-1} \tag{2.2}$$

It can be shown that

$$\frac{1}{2}\alpha(E) = -\sum_{\substack{k=1 \\ (k\ \text{odd})}}^{\infty} \frac{\mu_k(E)}{E^{k+1}} + \sum_{\substack{j=1 \\ (j\ \text{odd})}}^{\infty} \mu_j(E) E^{j-1} \tag{2.3}$$

where the μ's are given by

$$\mu_k(E) = \sum_{E_n<E} |\langle n \mid Q \mid 0\rangle|^2 E_n^k \tag{2.4a}$$

and

$$\mu_{-j}(E) = \sum_{E_n>E} |\langle n \mid Q \mid 0\rangle|^2 / E_n^j \tag{2.4b}$$

$|0\rangle$, $|n\rangle$ denote ground and excited states of the system. $\mathcal{E}_0, E_n$ denote ground state and excitation energies. Introducing

$$m_{-j} \equiv \mu_{-j}(E \to 0) \tag{2.5a}$$

$$m_k \equiv \mu_k(E \to \infty)$$

one can see that the static $\alpha(E \to o)$, instantaneous $\alpha(E \to \infty)$ response is characterized by the set of odd negative, positive moments m_k of the strength distribution $S(E)$ respectively

$$S(E) = \sum_n |\langle n | Q | 0 \rangle|^2 \delta(E - E_n) \tag{2.6}$$

$$m_k = \int_0^\infty S(E) E^k dE = \sum_n E_n^k |\langle n | Q | 0 \rangle|^2 \tag{2.7}$$

$$\alpha(E \to 0) = 2(m_{-1} + E^2 m_3 + \ldots) \tag{2.8}$$

$$\alpha(E \to \infty) = -\frac{2}{E^2}\left(m_4 + \frac{m_5}{E^2} + \ldots\right) \tag{2.9}$$

One can make similar considerations in terms of the Fourier transform $F(t)$ of the strength function [10]

$$S(E) = \frac{1}{2\pi}\int_{-\infty}^{+\infty} dt\ e^{-itE} F(t) \tag{2.10}$$

where the characteristic function $F(t)$ is given by

$$F(t) = \sum e^{itE_n} |\langle n|Q|0\rangle|^2 = m_0 + \frac{it}{1!} m_1 + \frac{(it)^2}{2!} m_2 + \ldots \tag{2.11}$$

Dispersion relations can be written connnecting the real and imaginary part of $F(t)$. One can then eliminate Re $F(t)$ and eq. (2.10) becomes

$$S(E) = \frac{2}{\pi}\int_0^\infty dt\ \sin Et\ \mathrm{Im}\ F(t) \tag{2.12}$$

which again involves only odd moments. In what follows we shall deal mainly with the quantities m_k, with k an arbitrary integral and Q a 1-body hermitian operator (a multipole operator). One can also write, for k integer and positive, m_k as a ground state expectation value

$$m_0 = \langle 0 \mid Q^2 \mid 0 \rangle \tag{2.13}$$

$$m_k = (-1)^t (i)^k \langle 0 \mid Q_s . Q_t \mid 0 \rangle \tag{2.14}$$

with

$$Q_s = [iH, [iH, \ldots, [iH, Q]\ldots]] \tag{2.15}$$

where s is the number of times that H appears in (2.15) and s,t are arbitrary integers but such that s + t = k. For the odd moments, eq. (2.14) can also be written as

$$m_k = \frac{1}{2} (-)^t (i)^k \langle 0 \mid [Q_s, Q_t] \mid 0 \rangle \tag{2.16}$$

which provides a useful simplification : $[Q_s, Q_t]$ leads to a (k + 1)-body operator. In contrast, the even moments are written in terms of anticommutators [4] and are thus (k + 2)-body operators. When Q commutes with the 2-body interaction V (Q isoscalar, V momentum independent) the many-body character of the operators in eq. (2.16) gets simpler. Q_1 is then a 1-body operator and the situation is illustrated on table 1. Some moments, marked with an asterisk in table 1, shall be discussed in section 4 : m_0 and m_1 for the electric dipole mode (Q_1 ~ 2-body) ; m_1 and m_3 for electric isoscalar monopole and quadrupole modes (Q_1 ~ 1-body).

The more widely used sum-rule is the linear energy weighted one (often referred toas EWSR)

$$m_1 = \sum_n E_n |\langle n \mid Q \mid 0 \rangle|^2 = \frac{1}{2} \langle 0 \mid [Q, [H, Q]] \mid 0 \rangle = m_1^T + m_1^V \tag{2.17}$$

where m_1^T, m_1^V denote the kinetic, potential contribution to m_1 respectively. If $Q = \sum q(\vec{r}_i)$ one has

$$m_1^T = \frac{\hbar^2}{2m} A(\vec{\nabla} q)_0^2 \qquad (2.18)$$

where $(\vec{\nabla} q)_0^2$ is the ground state expectation value.

- Monopole case $q = r^2$

$$m_1^T = \frac{2\hbar^2}{m} A r_0^2 \qquad (2.19)$$

where r_0^2 is the ground state mean square radius

- Quadrupole case $q = r^2 - 3z^2$

$$m_1^T = \frac{4\hbar^2}{m} A r_0^2 \qquad (2.20)$$

If the interaction contains no velocity dependent term contributing to m_1, then $m_1 = m_1^T$ and can be extracted directly from the experimental knowledge of r_0^2.

- Dipole case (with respect to center of mass R)

$$\vec{D} = \sum_{i=1}^{Z} (\vec{r}_i - \vec{R}) = \frac{1}{2} \sum_{i=1}^{A} \vec{r}_i \tau_3(i) - \frac{1}{2A} \left(\sum \tau_3(i) \right) \left(\sum \vec{r}_i \right) \qquad (2.21)$$

$$m_1(D_z) = \frac{\hbar^2}{2m} \frac{NZ}{A} + m_1^V = \frac{\hbar^2}{2m} \frac{NZ}{A} (1+\kappa) \qquad (2.22)$$

where the dipole enhancement factor κ is given by

$$\kappa = \frac{m}{\hbar^2} \frac{A}{NZ} \langle 0 | [D_z, [V, D_z]] | 0 \rangle \qquad (2.23)$$

κ is different from zero only if the interaction is velocity dependent and / or contains exchange terms like $\tau_+(i)\ \tau_-(j)$ which do not commute with the dipole operator.

Among the inverse energy weighted moments, only the m_{-1} moment will be discussed. It gives the static polarizability

$\alpha \equiv \alpha(E = 0)$ or zero frequency response and can be obtained by studying the response of the nucleus to a weak static external field $H - \lambda Q$. It is given by

$$\frac{1}{2}\alpha = m_{-1} = \frac{1}{2}\left.\frac{d\langle Q\rangle}{d\lambda}\right|_{\lambda=0} = \frac{1}{2}\left.\frac{d^2\langle H\rangle}{d\lambda^2}\right|_{\lambda=0} \qquad (2.24)$$

where the expectation value is taken with respect to the ground state of $H - \lambda Q$.

From the knowledge of several moments various quantities with dimensions of energy can be constructed, for instance

$$\tilde{E}_k \equiv (m_k / m_{k-2})^{1/2} \qquad (2.25)$$

and

$$\bar{E}_k \equiv m_k / m_{k-1} \qquad (2.26)$$

They statisfy the inequalities

$$\ldots > E_k > \tilde{E}_k > E_{k-1} > \tilde{E}_{k-1} > \ldots \qquad (2.27)$$

The equality signs in (2.27) hold when the strength is concentrated at a single energy (case of maximum collectivity). The closer the different $\tilde{E}_k$, $\bar{E}_k$ lie, the more concentrated in energy the strength function will be. Let us emphasize that there is no special merit in calculating the centroid energy m_1/m_0. Rather the natural procedure is to select the moments that can be computed more reliably and then, by eq. (2.27) or similar relations, give bounds on the quantities one is interested in.

By properly choosing the value of k in m_k (positive or negative), more emphasis can be put on the low or high energy part of the strength function. For instance, in the dipole case, the static polarizability (m_{-1}) is unsensitive to the high energy tail of the photonuclear cross-section. On the contrary the integrated photoabsorption cross-section, which is proportional to m_1, gets a sizable contribution from it.

Let us finally mention that it may be very useful to derive more general sum-rules than the ones considered in this talk. One can define

$$m_k(A, B) = \frac{1}{2}\sum_n E_n^k \left(\langle 0|A|n\rangle\langle n|B|0\rangle + \langle 0|B|n\rangle\langle n|A|0\rangle\right) \qquad (2.28)$$

The sum-rules we consider correspond to A = B (a multipole operator) and when there is no ambiguity we use the notation $m_k(A,A) = m_k(A) = m_k$. Several authors [4, 12-15] have considered the case k = 1 in (2.28). One has, for instance

$$m_1(\rho(\vec{r}), \rho(\vec{r}')) = \frac{1}{2}\langle 0|[\rho(\vec{r}), [H, \rho(\vec{r}')]]|0\rangle = \qquad (2.29)$$
$$= \frac{\hbar^2}{2m}\nabla_r \cdot \nabla_{r'}(\delta(\vec{r}-\vec{r}')\langle 0|\rho(\vec{r})|0\rangle)$$

where $\rho(\vec{r}) = \sum \delta(\vec{r}-\vec{r}_i)$ is the density operator. For many purposes it is convenient to write (2.29) in momentum space

$$m_1(\rho_{\vec{k}}, \rho_{-\vec{q}}) = \frac{1}{2}\langle 0|[\rho_{\vec{k}}, [H, \rho_{-\vec{q}}]]|0\rangle = \qquad (2.30)$$
$$= \frac{\hbar}{2m}\vec{k}\cdot\vec{q}\,\langle 0|\rho_{\vec{k}-\vec{q}}|0\rangle$$

where $\rho_{\vec{k}} = \sum \exp(-i\vec{k}\cdot\vec{r}_i)$. Introducing the multipole operators Q^λ

$$Q^{\lambda} = \int r^{\lambda}\, Y_{\lambda_0}(\hat{r})\, \rho(\vec{r})\, d\vec{r} \qquad (\lambda \neq 0) \qquad (2.31)$$

$$Q^{0} = \int r^{2}\, \rho(\vec{r})\, d\vec{r}\ , \qquad (2.32)$$

and the form factors

$$F^{\lambda}(q) = [4\pi(2\lambda+1)]^{1/2} \int j_{\lambda}(qr)\, Y_{\lambda_0}(\hat{r})\, \rho(\vec{r})\, d\vec{r}\ , \qquad (2.33)$$

with the elastic form factor defined by

$$F_{el}(q) \equiv \langle 0 | F^{\lambda=0}(q) | 0 \rangle \qquad (2.34)$$

and using that the isoscalar density commutes with the interaction, one obtains by perfoming the appropriate integrations, for instance

$$m_1(\rho, Q^{\lambda}) = -\frac{h^2}{2m}\, \lambda r^{\lambda-1}\, \frac{d\rho_{00}(\vec{r})}{dr}\, Y_{\lambda_0}(\hat{r}) \quad (\lambda \neq 0) \qquad (2.35a)$$

$$m_1(\rho, Q^{0}) = -\frac{h^2}{m}\, (3 + r\frac{d}{dr})\, \rho_{00}(\vec{r}) \qquad (2.35b)$$

$$m_1(Q^{\lambda}, F^{\lambda}) = (-)^{\lambda+1}\, \frac{h^2}{2m} \lambda(2\lambda+1) q^{\lambda} \left(\frac{1}{q}\frac{1}{dq}\right)^{\lambda-1} F_{el}(q) \quad (\lambda \neq 0) \qquad (2.36a)$$

$$m_1(Q^{0}, F^{0}) = \frac{h^2}{2m}\, q \frac{d}{dq} F_{el}(q) \qquad (2.36b)$$

$$m_1(Q^{\lambda}) = \frac{h^2}{2m}\, \lambda(2\lambda+1) \frac{1}{4\pi}\, A\, r_0^{2\lambda-2} \quad (\lambda \neq 0) \qquad (2.37a)$$

$$m_1(Q^{0}) = \frac{2h^2}{m}\, A\, r_0^{2} \qquad (2.37b)$$

Eqs. (2.35) relate sum-rules involving transition densities to the ground state density. The r.h.s. of (2.35) is identical to the

transition densities obtained through specific nuclear models, e.g. by Tassie [16], following the hydrodynamical description of an irrotational fluid. Eqs.(2.36) relate sum-rules involving transition form factors to the elastic form factor. Eqs.(2.35) are the familiar sum-rules for multipole matrix elements, relating them to the ground state expectation value of r^n ; they are particular cases of the more general relation (2.18). All these sum-rules are particularly easy to exploit when, for a given multipolarity, they are dominated by a single collective state. In this case, for instance, all the form factors become proportional to each other [13] and the transition density of the state dominating the sum-rule coincides with the one obtained by Tassie.

3. Experimental systematics on electric giant resonances.

A great deal of information on the dipole strength comes from photonuclear data [17-22, 48]. There are two main sources :

i) neutron emission cross-sections (γ, xn). The sum of all the partial neutron cross-sections gives practically the total cross section for heavy nuclei because in that case the (γ, p) contribution is very small due to the Coulomb barrier. For light nuclei, the photonuclear cross-sections will give only a fraction of the total cross section.

ii) total absorption cross-sections. One must extract from the data the nuclear contribution from the total measured cross-section. The non-nuclear part increasing rapidly with Z, this method has been used only for light nuclei ($A \leq 40$).

For these reasons, both methods are complementary but unfortunately it has not been possible to make a direct test on the consistency of data extracted by the two techniques.

Most of the information concerning the isoscalar quadrupole and monopole modes comes from inelastic hadron scattering (p, d, ^{3}He and α) with projectile energies of the order of 100 Mev. To extract nuclear structure information one must make specific assumptions for the nuclear reaction process (direct reaction) and for the transition densities. As a consequence the parameters derived when analyzing the data are by far less reliable than for the photonuclear case. This remark

applies especiallly to the percentage of EWSR for the isoscalar monopole mode.

3.1 Dipole case (GDR).

On fig.1 are plotted the data corresponding to the energy E_D of the giant dipole resonance. They can be well reproduced by (see fig.1 b)

$$E_D \simeq 79\, A^{-1/3}\ \text{Mev} \qquad (3.1)$$

However a similar agreement can be obtained with $E_D \simeq$ const. $A^{-1/6}$ Mev, as shown on fig.1 a . Let us remind that a $A^{-1/3}$ -law is obtained [5] in the hydrodynamic model for the motion of neutron versus protons, motion in which the boundary of the nucleus remains unchanged (Steinwedel - Jensen volume mode). For the motion of neutrons as a whole versus protons as a whole (Goldhaber - Teller surface mode) a $A^{-1/6}$ -law is obtained (see ref.[47] for a hydrodynamical description in which this two modes are coupled).

The data on the widths are reproduces on fig.2 a. They lie between 4 and 7 Mev and show pronounced deformation and shell closure effects.

It is customary to discuss the following integrated quantities extracted from the total photoabsorption cross-section $\sigma(\omega)$

$$\sigma_p = \int \sigma(\omega)\omega^p\, d\omega \qquad p = 0,-1,-2 \qquad (3.2)$$

a) σ_0

Integrated cross-sections up to the pion threshold have been determined for light nuclei ($A \leq 40$) by total photon

absorption cross-section measurements [20]. Recently the $\sigma(\gamma,xn)$ cross-sections of five heavy nuclei (Sn, Ce, Ta, Pb and U) have been measured at Saclay with monochromatic photons of up to 120 Mev. In fig.3 are reproduced the data corresponding to lead showing a long tail, of the order of 10 to 20 mb [21, 22].

On fig.2 b are plotted values of σ_0 obtained by extrapolating $\sigma(\omega)$ with a Lorentz-curve that fits the measured cross-section in the giant resonance region. For medium and heavy nuclei one obtains $\kappa \simeq 0.3$ (see eqs.(2.3), (4.10)).On fig.4 are plotted the values of $1 + \kappa$ obtained from the photo-neutron cross-section measurements of heavy nuclei. Since it is often assumed that one can compare the dipole EWSR with experiment up to the pion threshold, a smooth extrapolation from 120 to 140 Mev has been made before extracting the value of the enhancement factor κ. One obtains $\kappa = 0.75 \pm 0.15$, independent on the mass number for $A \geq 8$. Also included on fig.4 are the Mainz values [20] for light nuclei, from total cross-section measurements.

The long tail of $\sigma(\omega)$ (see fig.3) beyond the GDR is largely due to medium or short range correlations, mainly induced by the tensor force [23]. Consequently, approaches like RPA that include only long range correlations and ignore the tensor force should produce, for heavy nuclei, values of $\kappa \simeq 0.2\text{-}0.4$, whereas theories that include short range tensor correlations should produce values of $\kappa \simeq 0.8\text{-}1.0$.

b) σ_{-1} (bremsstrahlumg weighted) and σ_{-2}

Some data are reproduced on table 2. The values in columns I come from total cross-section measurements, in

columns II from photoneutron cross-sections. The values for A >100, for which photoneutron data give reliably the total photo cross-section, are well reproduced by

$$\sigma_{-1} = (0.20 \pm 0.02)\ A^{4/3}\ \text{mb} \qquad (3.3)$$

$$\sigma_{-2} = (2.7 \pm 0.2)\ A^{5/3}\ \mu\text{b/Mev} \qquad (3.4)$$

3.2 Quadrupole isoscalar (GQR).

On fig.5 is reproduced the systematics on GQR [24] : energy, width and percentage of EWSR (m_1). The peak energy E_Q is well reproduced by

$$E_Q \simeq 63\ A^{-1/3}\ \text{Mev} \qquad (3.5)$$

with some tendency towards a slightly larger value for heavy nuclei.

The resonance width is of the order of 4-6 Mev, larger for very light systems, smaller for very heavy. For A≥ 100, the EWSR (eq.(2.20)) is exhausted by the measured strength. Probably that for the sum-rule depletion error bars larger than those of fig.5 would better reflect present uncertainties.

3.3 Monopole isoscalar (GMR).

Fig.6 summarizes the data obtained by inelastic deuteron scattering at 82 and 108 Mev at Orsay [25], inelastic α scattering at 96 Mev at Texas [26] , inealstic ^{3}He scattering at 108 Mev at Grenoble [27] and 60 Mev inelastic proton scattering at Oak Ridge [28]. Progress in determining monopole strength has been recently achieved mainly by

i) measuring cross sections at very small angles, where L = 0 and L = 2 angular distributions differ substantially, providing unambiguous L = 0 signature.

ii) reducing the background coming from particles rescattered by the spectrometers

Fig. 6a shows that the resonance peak E_M is well reproduced by

$$E_M \simeq 80 \; A^{-1/3} \text{ Mev} \qquad (3.6)$$

The resonance widths (fig.3b) are typically of the order of 3 Mev and a large fraction (fig. 3c) of the m_1 sum-rule (eq.(2.19)) is exhausted (remember that the methods used in extracting sum-rule depletions in hadron scattering are quite model dependent).

4. Evaluation of sum-rules

4.1 RPA sum-rules [11, 29-38]

Most of the sum-rule evaluations described in what follows will be RPA sum-rules, i.e. in analogy to eq.(2-7)

$$m_k(\mathrm{RPA}) = \sum (E_n)^k_{\mathrm{RPA}} \, |\langle n|Q|0\rangle_{\mathrm{RPA}}|^2 \qquad (4.1)$$

where $(E_n)_{\mathrm{RPA}}$, $\langle n|Q|0\rangle_{\mathrm{RPA}}$ are excitation energies, transition matrix elements corresponding to the RPA method. As is well known, the standard Time Dependent Hartree-Fock (TDHF) derivation of RPA specifies how to construct the response function and the RPA matrices from the effective interaction used in determining the ground state. We shall say that a RPA calculation is selfconsistent when it is performed by using this procedure. All the properties and theorems we shall discuss concerning sum-rules and RPA apply only to the selfconsistent RPA scheme.

a) m_1 (Thouless theorem [29])

If Q is a 1-body operator, then

$$m_1(\mathrm{RPA}) = \tfrac{1}{2}\langle\phi|[Q,[H,Q]]|\phi\rangle \qquad (4.2)$$

where ϕ denotes the Hartree-Fock (HF) solution. The RPA, in contrast to the Tamm-Dancoff approximation (TDA), preserves in the sense of eq.(4.2) the exact relation eq.(2.17). What is remarkable with this and related theorems is that, despite the fact that RPA contains dynamical ground state correlations, some RPA sum-rules (m_1 in this case) can be obtained as an expectation value with respect to the HF uncorrelated ground state.

b) m_3 (cubic energy weighted)

A relation similar to (4.1) holds

$$m_3(\text{RPA}) = \frac{1}{2}\langle\phi|[G,[H,G]]|\phi\rangle \tag{4.3}$$

where G is an operator which can be explicitely derived from the HF hamiltonian [36]. When $[V, Q] = 0$, eq.(4.3) reduces to [11,33]

$$m_3(\text{RPA}) = \frac{1}{2}\langle\phi|[Q_1,[H,Q_1]]|\phi\rangle \tag{4.4}$$

with Q_1 defined by eq.(2.15). This allows to interpret m_3 as a polarizability : "Scale" the HF wave function ϕ by

$$\phi \longrightarrow \phi(\eta) = e^{-i\eta Q_1}\phi \tag{4.5}$$

where η is a "scaling" parameter. Then

$$m_3(\text{RPA}) = \frac{1}{2}\frac{d^2}{d\eta^2}\langle\phi(\eta)|H|\phi(\eta)\rangle\Big|_{\eta=0} \tag{4.6}$$

in analogy to eqs.(2.24, 4.7). If $Q = Q^0$ is the monopole operator, the transformation (4.5) scales by the same factor each single-particle wave function. If $Q = Q^{\lambda=2}$ is the quadrupole operator, the transformation (4.5) induces the same volume preserving quadrupole transformation on each single-particle wave function.

c) m_{-1} (inverse energy weighted)

The static RPA polarizability can be obtained by [30, 31]

$$m_{-1}(\text{RPA}) = \frac{1}{2}\frac{d}{d\lambda}\langle\phi(\lambda)|Q|\phi(\lambda)\rangle\Big|_{\lambda=0} = \frac{1}{2}\frac{d^2}{d\lambda^2}\langle\phi(\lambda)|H|\phi(\lambda)\rangle\Big|_{\lambda=0} \tag{4.7}$$

where $\phi(\lambda)$ is the constrained HF solution of $H-\lambda Q$. Eq.(4.7) is the RPA version of the exact relation (2.24).

d) Dynamic polarizability $\alpha(E)$ [36]

More generally, it can be shown that the TDHF polarizability $\alpha_{TDHF}(E)$ satisfies

$$\alpha_{TDHF}(E) = \sum_n \left\{ \frac{|\langle n|Q|0\rangle_{RPA}|^2}{(E_n)_{RPA} + E} + \frac{|\langle n|Q|0\rangle_{RPA}|^2}{(E_n)_{RPA} - E} \right\} \qquad (4.8)$$

which is the TDHF analogue of eq.(2.1)

In what follows we shall compare to experimental data sum-rules evaluated by the methods just outlined. The results, depending as they do, on RPA theorems are of the same accuracy, in principle, as full RPA calculations. In practice they are superior to most existing RPA calculations, since these often contain lack of selfconsistency and/or basis truncation effects, in particular by ignoring continuum particle states. We show in fig.7 the monopole and quadrupole isoscalar strength from a selfconsistent RPA calculation which properly includes the continuum [39, 40] (see introduction, route n°1). The strength S(E) being a relatively smooth function of the energy, these results give additional support to the view that a very limited set of moments will reproduce essential features of the strength distribution and will contain systematic effects. When using sum-rules to locate collective strength in the case of a broad resonance, different definitions of energy ($\tilde{E}_k$'s, $\bar{E}$'s in eqs.(2.25, 2.26)) will differ considerably yet still being consistent (for instance the monopole isoscalar case of ^{16}O on fig.7). When the resonance is narrow (the other cases on fig.7) the different definitions lie much closer together. To illustrate this point, arrows

on fig.7 show values of $\tilde{E}_1$ and $\tilde{E}_3 (\tilde{E}_1 < \tilde{E}_3)$ for the monopole case. The arrows for the quadrupole case indicate the value of $\tilde{E}_3$. The different $\tilde{E}$'s have been calculated by the techniques described above [11, 33] and are consistent with the complete calculation of ref.[39, 40].

Most of the results we shall discuss are obtained with effective interactions, in particular of the Skyrme type [41, 42]. The simplicity of these interactions (zero range) is such that analytical results can be obtianed in some cases, giving more physical insight. Their parameters have been fitted to observed bulk properties of ground states (total binding energies, radii) given by the HF method. They contain momentum dependent terms that induce a non-locality of the average field (i.e. an effective mass m^*) and take into account finite range effects. Despite of the velocity dependence, one still has $[V, Q] = 0$ when Q is an isoscalar operator. For isovector operators, the velocity dependent terms contribute to the commutator and immitate closely the effects of a charge-exchange force. Like more realistic effective forces, Skyrme interactions contain a two-body density dependent term. Specifically

$$V(\vec{r}_1, \vec{r}_2, \rho(\vec{r}_1), \rho(\vec{r}_2)) = \frac{1}{6} t_3 (1+X_3 P_\sigma) \rho^\gamma (\vec{r}_1) \delta(\vec{r}_1 - \vec{r}_2) \qquad (4.9)$$

Choices in the literature are $\gamma=1$ [41,42], $\gamma=2/3$ [43], $\gamma=1/3$ [44], $\gamma=1/6$ [45,46].

When dealing with density dependent forces care must be taken in properly defining the RPA matrices and the proof of Thouless and related theorems requires further elaboration but they still hold [11, 38].

4.2 Comparison with experiment.

4.2.1. Dipole case.

We shall discuss separately the integrated photoabsorption cross-sections (3.2). If higher multipole contributions and finite wavelength modifications are ignored, they are given by the sum-rules

$$\sigma_p = 4\pi^2 \frac{e^2}{\hbar c} m_{p+1} \quad (D_z) \qquad p = 0, -1, -2 \qquad (4.10)$$

where the dipole operator $\vec{D}$ is given by (2.21). It can also be written

$$\vec{D} = \frac{NZ}{A} \vec{r}_{ZN} \qquad (4.11)$$

where $\vec{r}_{ZN} = \vec{R}_Z - \vec{R}_N$ is the relative coordinate of the center of mass of protons with respect to the center of mass of neutrons. Consequently, in the dipole approximation, the only quantities relevant to photoabsorption are the ones connected with the relative motion of the c.m. of protons with respect to the c.m. of neutrons. Let us assume that this motion is decoupled and that its hamiltonian H_{ZN} is

$$H_{ZN} = \frac{p^2}{2\mu} + \frac{1}{2} \mu \Omega^2 r_{ZN}^2 \qquad (4.12)$$

where $\mu = (NZ/A)m$. One has $E_D = \hbar\Omega$, $\sigma_0 = 60(NZ/A)$ Mev.mb, $\sigma_{-1} = \sigma_0/\hbar\Omega$ and $\sigma_{-2} = \sigma_0/(\hbar\Omega)^2$ [50]. The harmonic oscillator independent particle model (HOSM) gives $\hbar\Omega = \hbar\omega$ where $\hbar\omega$ is the frequency of the HOSM [49]. One gets (taking $\hbar\omega \simeq 41\ A^{-1/3}$ Mev and $NZ/A \simeq A/4$)

$$E_D = 41 A^{-1/3} \text{ Mev}, \quad \sigma_{-1} = 0.37\ A^{1/3} \text{ mb}, \quad \sigma_{-2} = 8.92\ A^{5/3} \ \mu\text{b}\cdot\text{Mev}^{-1} \qquad (4.13)$$

in disagreement with the experimental values (3.1), (3.3) and (3.4). If one takes in (4.11) $\hbar\Omega = 79\ A^{-1/3}$ Mev in order to reproduce the observed giant resonance energy (3.1) one has

$$E_D = 79\ A^{-1/3}\ \text{Mev},\quad \sigma_{-1} = 0.19\ A^{5/3}\ \text{mb},\quad \sigma_{-2} = 2.4\ A^{5/3}\ \mu\text{b.Mev}^{-1} \tag{4.14}$$

in good agreement with the data for heavy nuclei. So, to get agreement with experiment for E_D, σ_{-1} and σ_{-2} one has simply to change the frequency of the relative motion of protons with respect to neutrons from the value produced by the independent particle model ($\hbar\omega$) to approximately twice this value. The question now is : Are usual microscopic theories of collective motion, like TDA or RPA, successful in this respect ? Before embarking ourselves in more ambitious and selfconsistent treatments wich, in particular, take exchange effects into account, let us look to what one can expect from simple approaches. Specifically, let us consider the predictions of the degenerate schematic model [51, 52]. If the coupling constant is adjusted in order to give $\hbar\Omega_{RPA} = \hbar\Omega_{TDA} = \hbar\Omega$ (observed collective frequency), one has

$$\frac{\sigma_{-1}(\text{TDA})}{\sigma_{-1}(\text{RPA})} = \frac{\hbar\Omega}{\Delta\epsilon} = \frac{\hbar\Omega}{\hbar\omega} \simeq \frac{79}{41} \tag{4.15}$$

where $\Delta\epsilon = \epsilon_p - \epsilon_h$ is the particle-hole energy. The TDA value of σ_{-1} ($\sim\langle 0|D^2|0\rangle$, see (4.10)) corresponds to an independent particle evaluation, should therefore be identified to the one given by (4.13) and will be in disagreement with the data. On the

contrary, from (4.15) one can see that σ_{-1} (RPA) will coincide with (4.14) and agree with the data. In summary :

i) photoabsorption is only sensitive to the relative motion of protons as a whole with respect to neutrons as a whole [49, 50]. This simple observation invalidates, for instance, previous attempts to extract the mean square radius from the integrated cross-section σ_{-1} ;

ii) the data indicate that this relative motion has a frequency which is twice the one predicted by the independent particle model, which includes only Pauli correlations [50] (equivalently, the amplitude of dipole oscillations is smaller than the one predicted by the independent particle model) ;

iii) the schematic model indicates that, in contrast to TDA, the ground state long range correlations included in RPA produce precisely the effect indicated in ii).

Let us now discuss results obtained in selfconsistent approaches, specifically complete RPA calculations with Skyrme forces [39, 40, 53, 54] as well as some sum-rule evaluations [32, 55-57]. The calculated cross-sections show, in comparison with the data, too much structure and only after smoothing the computed cross section can one reproduce the experimental peak [54]. Commonly used Skyrme forces give some additional strength beyond the resonance that has no experimental counterpart, feature which is not well understood. There are good indications [46] that the parameters of Skyrme-type forces can be modified in such a way that, keeping agreement with bulk

properties, the dipole (and other multipole) strength is better reproduced. Remember also that from a variety of analysis (see for instance [17, 46, 47]) one can conclude that the volume symmetry energy in nuclear matter at the saturation density is by no means the only relevant parameter in determining the dipole strength.

a) σ_0

In section 4.3 will be discussed results of evaluations of the enhancement factor κ (eqs.(2.23), (4.10)) with realistic forces. Let us now only mention that, as should be clear from the discussion of section 3.1, Skyrme-type forces should produce values of κ of the order of 0.2-0.4. For these forces the expression of κ is

$$\kappa = \frac{m}{2\hbar^2}\frac{1}{A}\,(t_1 + t_2)\int \rho^2(\vec{r})\,d\vec{r} \qquad 4.16)$$

where ρ is the ground state density and t_1 and t_2 are the parameters that govern the momentum dependence of the interaction. For lead, the values corresponding to S III [42], SkM [46] and Ska [44] are 0.42, 0.37 and 0.69 respectively [46]. This last value indicates that the Ska force fails in reproducing correctly the dipole strength. As we shall later see, the polarizability predicted by this force is indeed in disagreement with the experimental data.

b) σ_{-1}

Dellafiore and Brink [50] have given a beautiful model- independent interpretation of σ_{-1}

$$\sigma_{-1} = \frac{4}{3}\pi^2 \frac{e^2}{\hbar c}\left(\frac{NZ}{A}\right)^2 <0|r_{ZN}^2|0> \qquad (4.17)$$

which follows immediately from (4.10) and (4.11). Eq.(4.17) tells that σ_{-1} is a direct measure of the Goldhaber-Teller (GT) zero-point motion. As pointed out in ref.[48], the amplitude of this motion is surprisingly large for light nuclei. We illustrate this point in table 3. From the experimental knowledge of σ_{-1} (first column) is extracted the value of $<r_{ZN}>^{1/2}$ (second column) by use of relation (4.17). The ratio $\mathcal{R}$ of the zero-point GT root mean square radius to the charge root mean square radius r_c (third column)

$$\mathcal{R} = \left(\frac{<0 \mid r_{ZN}^2|0>}{r_c^2}\right)^{1/2} \qquad (4.18)$$

is given in the fourth column. The fifth column gives the following estimation of $\mathcal{R}$: take (4.12) to describe the relative proton-neutron motion, with $\hbar\Omega = 79A^{-1/3}$ Mev, $\mu = (A/4)m$, the h.o. 1s state for the zero-point motion and $r_c^2 = 0.9A^{2/3}$ fm^2. One obtains $\overline{\mathcal{R}} = 1.87\ A^{-2/3}$, in very good agreement with the value of $\mathcal{R}$ extracted from experiment. The last column ($\mathcal{R}_{GDR} = \sqrt{5/3}\ \mathcal{R}$) corresponds to the ratio of the root mean square radius of the proton-neutron motion of the giant resonance (relative motion in the 1ρ state) to the ground state charge root mean square radius.

For light nuclei, where $\mathcal{R}$ and $\mathcal{R}_{GDR}$ are large, there are good chances that proton and neutron distributions have a relatively small overlap, as sketched on fig.8. One can then

imagine that the study of the deexcitation of the GDR of light systems may provide information on, for instance, neutron-neutron correlations. In particular, the possibility to observe multineutron bound states in this way should be explored (in ^{7}Li, for which β_{GDR} is 0.68, the 2n and 3n thresholds are in the giant resonance region).

For p = -1, eq.(4.10) reads

$$\sigma_{-1} = 4\pi^2 \frac{e^2}{\hbar c} \langle 0|D_Z^2|0\rangle, \qquad (4.19)$$

the experimental knowledge of σ_{-1} providing thus a direct measure of the ground state expectation value of a two-body operator (see also table 1) and giving direct information on two-body correlations. Furthermore, as discussed above and emphasized in ref.[58], the value of $\langle 0|D_Z^2|0\rangle$ obtained from a correlated and non-correlated ground state wave function is very different. As Lane and Mekjian say, "there are remarkably few examples in nuclear physics where one can pinpoint the effect of correlations in so explicit a way... The only other case is that of the total energy where the operator is the hamiltonian". In fact, as we shall see in section 4.4 when dealing with σ_0, the enhancement factor κ provides, with some qualifications, another case.

On table 4 comparison is made, for ^{16}O and ^{208}Pb of the experimental and computed RPA values of σ_{-1}, and a very good agreement is achieved with the Mainz value of ^{16}O and the Saclay value of ^{208}Pb. The RPA value is evaluated by means

of eq.(3.2), after computing the entire dipole strength distribution, since there is no direct way to obtain even RPA sum-rules [35] ($m_0(D_Z)$ in this case). The experimental value for lead, when the giant dipole resonance is Lorentz extrapolated and the contribution below 7.3 Mev is estimated [58], is corrected from 0.19 to 0.22 which coincides (accidentally !) with the computed value . Let us emphasize that the agreement with experiment for light (^{16}O) and heavy (^{208}Pb) nuclei gives a very strong indication that values extracted from photoabsorption data for light nuclei and photoneutron data for heavy nuclei are consistent. One can finally conclude that the ground state dipole correlations deduced from experiment are large and well reproduced by selfconsistent RPA approaches

c) σ_{-2}

From (4.10) and (2.24) one has

$$\sigma_{-2} = 2\pi^2 \frac{e^2}{\hbar c}\ \alpha_D = 4\pi^2 \frac{e^2}{\hbar c}\ m_{-1}(D_Z) \qquad (4.20)$$

where α_D is the static dipole polarizability. It has been computed [56] using the HF method with an applied external dipole field (eq.(4.7)). Results corresponding to several forces are presented on table 4. Although they depend on the interaction used, one can see, by comparing to the experimental values, that they roughly reproduce the Mainz values for light nuclei and the Saclay values for heavy nuclei. So, before going into a more detailed analysis, one can get two main conclusions : 1) photoneutron data for light nuclei do not provide an estimate of σ_{-2} ; 2) the calculations indicate that contrarily to what has been

concluded by other authors, the σ_{-2} values (as well as σ_{-1}) extracted from photoabsorption data for light nuclei and from photoneutron data for heavy nuclei are consistent in the sense that the same theoretical scheme (selfconsistent RPA) reproduces both.

It is popular in the literature to give values of σ_{-2} referred to Migdal's estimate of the polarizability, which reads [59, 1]

$$\sigma_{-2} = 2\pi^2 \frac{e^2}{\hbar c} \frac{R^2 A}{40\, a_\tau} \quad , \tag{4.21}$$

where R is the sharp nuclear radius and a_τ is the volume symmetry energy coefficient appearing in the Weizsäcker formula. Values obtained through eq.(4.21) are given at the bottom of table 4 where the values of a_τ corresponding to each force are also included. As can be seen, (4.21) does not provide a good estimate of σ_{-2} and the correlation between values of σ_{-2} and a_τ predicted by (4.21) is not correct. Agreement of eq.(4.21) with the data for heavy nuclei could be achieved by taking $a_\tau \simeq 20$ Mev but this value is very far from the ones obtained from forces that describe correctly bulk properties as well as from the value obtained in the liquid droplet model ($a_\tau = 36.8$) [60]. In fact, the inadequacy of (4.21) is not surprising, for the dipole mode cannot be described simply as a volume mode. As pointed out in refs.[46, 47], surface effects are very important and the most relevant parameters are the volume and surface (stifness coefficient against formation of neutron skin) symmetry energy coefficients. Also included on the last column of table 4 is a lower bound of σ_{-2} obtained by sum-rule techniques [32, 37, 55].

By comparing results of the last two columns, which are obtained with the same force, one can see that the bounds are 5-15% lower than the exact RPA values and provide an efficient and simplified way to estimate the dipole polarizability. Comparison of results obtained with different forces with experimental values show that Ska force does not describe correctly dipole properties and that SkM force is slightly better than Skyrme forces. The predicted values for ^{90}Zr are too high compared to the photoneutron value. However for this nucleus the (γ, p) channel would probably still give a sizable amount to the total cross-section and increase σ_{-1}. We think that the comparison between calculated and observed values cannot be pushed further until an estimation of the error bars attached to the values extracted from photoabsorption cross-sections is given.

4.2.2. Quadrupole case. (see [11] and references therein)

We shall use to estimate the energy E_Q of the giant quadrupole resonance the quantity $\tilde{E}_3$ (see eq.(2.25)) that can be computed using eqs.(4.2) and (4.6) with $Q \approx \sum(r_i^2 - 3z_i^2)$. For Skyrme-type forces one obtains

$$E_Q \simeq \left(\frac{4\hbar^2\ T}{m\ A\ r_0^2}\right)^{1/2} \left(1 + \frac{E_{fin}}{T}\right)^{1/2} , \qquad (4.22)$$

where r_o^2 is the mean square radius, T is the total kinetic energy of the ground state and E_{fin} (finite range term) is the contribution to the ground state energy arising from the momentum dependent terms of the interaction (terms that give rise to an effective mass). One can show that E_{fin}/T is almost independent of A and therefore the quantity $1 + E_{fin}/T$ can be estimated by taking the limit of a large system, in which case it tends to

m/m^*, where m^* is the nuclear matter effective mass,

$$E_Q \simeq \left(\frac{4\hbar^2 T}{m\ A\ r_0^2}\right)^{1/2} \sqrt{\frac{m}{m^*}} \qquad (4.23)$$

If one estimates T/r_0^2 by its harmonic oscillator value, one obtains

$$E_Q \simeq \sqrt{2}\ \hbar\omega \sqrt{\frac{m}{m^*}} \qquad (4.24)$$

When $m/m^* = 1$ one recovers the Suzuki- Mottelson result. Introducing the experimental information on the energy of the giant quadrupole resonance (eq.(3.5)) one obtains the following estimation of the nuclear matter effective mass

$$\frac{m^*}{m} \simeq 0.75 - 0.85 \qquad (4.25)$$

Several authors have performed this type of analysis reaching similar conclusions. In ref.[61] a slightly larger value of m^*/m than the one provided by eq.(4.25) is obtained. In ref.[38], $\tilde{E}_3$ is computed for ^{16}O and ^{40}Ca with the finite range density dependent interaction Go of Campi-Sprung.

Our main conclusion is that if the quadrupole strength is highly collective, the knowledge of the energy E_Q of the quadrupole resonance can be used to estimate the nuclear matter effective mass m^*.

4.2.3. Monopole case (see [11] and references therein)

The study of the giant monopole resonance is of special interest. It corresponds to the "breathing" or compression -

dilatation mode and its frequency provides information on the incompressibility of nuclear matter, a parameter of central dynamical interest that otherwise can be reached only rather indirectly. For nuclear matter, the incompressibility K_{nm} is defined unambiguously as

$$K_{nm} = k_F^2 \frac{d^2 E/A}{dk_F^2}\Big|_{k_F=k_{F_o}} \qquad (4.26)$$

where E/A is the energy per particle and k_F (k_{F_o}) is the Fermi momentum (Fermi momentum at saturation density) . For finite nuclei there is no unique definition of incompressibility : the response of the nucleus will depend on the form of the applied monopole field. We shall consider $Q = \sum r_i^2$ and shall discuss the properties of the compression modulus K_A associated to "scaling" (see eq.(4.6)), in which case

$$K_A = \frac{1}{2A}\left(\frac{m}{\hbar^2}\right)^2 m_3 \qquad (4.27)$$

where m_3 is given by (4.4) or (4.6). This procedure will be more sensible the more concentrated in energy the strength distribution is. Explicit calculations show indeed that the monopole strength for $Q = \sum r_i^2$ is concentrated in energy for heavy nuclei (see fig.7). Using again to estimate the monopole energy E_M the quantity $\bar{E}$, , one has, using (4.2) and (4.4) or (4.6)

$$E_M \simeq \frac{\hbar}{r_0}\sqrt{\frac{K_A}{m}} \qquad (4.28)$$

The experimental position of the monopole resonance (eq. (3·6)) gives, by use of (4·28), $K_A \simeq 150$ Mev. For Skyrme-type forces one can furthermore show that

$$K_{nm} - K_A \simeq 63(1+\gamma) \text{ Mev} \qquad (4.29)$$

where γ is defined in eq. (4·9). Due to the limited number of parameters of Skyrme-type forces, the effective mass m^* and the incompressibility are related and using the constraint (4·25) on the effective mass put by the data in the quadrupole resonance one deduces that, in order to reproduce the experimental information, one must take $\gamma \simeq \frac{1}{3} - \frac{1}{6}$ and by use of (4·29) one obtains for the nuclear matter incompressibility $K_{nm} \simeq 220$-230 Mev. Explicit calculations of $\tilde{E}_3$ confirm this analysis and in ref.[46] a Skyrme-type force with $\gamma = \frac{1}{6}$ and $K_{nm} = 220$ Mev has been constructed that keeps agreement with bulk properties and reproduces correctly quadrupole, monopole and dipole resonances.

It is worthwile to mention that Blaizot et al. [61, 62] in their study of monopole resonances using RPA reach also the conclusion that present data require $K_{nm} \simeq 210 \pm 30$ Mev. Finally, Myers and Swiatecki [60], using a completely different approach-macroscopic description of binding energies - obtain for the nuclear matter incompressibility a value of 240 Mev. We believe that the convergence, using different methods that include different experimental information, towards values of $K_{nm} \simeq 200$-240 Mev is a very significant result. It should be used in the future to test effective nucleon-nucleon interactions as well as many-body theories of nuclear matter.

4.3 The dipole enhancement factor κ.

Let us now separately discuss what can be learned from the experimental knowledge of σ_0, using methods that go beyond RPA and that use realistic two-body forces. In contradistinction to σ_{-1} and σ_{-2}, for which the energy weighting facilitates the comparison with finite energy evaluations, for σ_0 there is no clear cut relation between the experimental value up to pion threshold and the Thomas-Reiche-Kuhn (TRK) evaluation (evaluation given by eqs.(2.22), (2.23) and (4.10)). Some general remarks are in order here [9, 63, 64] :

i) the evaluation of the double commutator with the conventional nuclear physics includes photoabsorption also above pion threshold

ii) there is considerable, although not complete, cancellation of dipole retardation effects against higher multipoles

iii) there are contributions from the subnucleonic level, isobaric and meson exchange currents.

From detailed studies performed mainly for the deuteron, one expects that the TRK value should slightly exceed the experimental measured photoabsorption cross-section integrated up to pion threshold. More work in this direction is needed before a more quantitative statement can be made.

That the TRK value may be interesting in order to compare different many-body approaches is based on the fact that the double commutator (2.23) is a two-body operator (see table 1). Consequently, the value of κ depends on the two-body

correlations of the wave function induced by the hamiltonian. In section 4.2.1 we have seen that for σ_{-1} too the two-body correlations come into play. However, for the later case it is mainly the long range correlations that modify the independent particle value. For κ , on the contrary, the interaction appears explicitely and the weighting provided by the interaction in matrix element of r^2V emphasizes an intermediate range of 1 to 2fm, where the defect wave function is still appreciable. Furthermore, the presence of the tensor force in r^2V allows a coupling of channels that is very important and no analogous process occurs for σ_{-1} [65] .

On table 5 are reproduced the results of several calculations of the TRK value of κ using realistic forces, Hamada-Johnston (HJ) and Reid soft core (RSC) potentials. Also included for comparison are the experimental values (see section 3.1). The experimental value for ^{6}He is obtained by adding the contributions of known decay channels and is probably unreliable. The calculations for A = 2 and 3 contain no uncertainties (the exact non-relativistic problem is solved, using Fadeev equations for A = 3) and different authors obtain essentially identical results [64 ,66-68] . Several methods have been used for heavier nuclei : first-order perturbation theory to estimate tensor effects in ref.[69] , a linked expansion of the expectation value (2.23) involving the Bethe-Goldstone wave function in ref.[70] , the expS method in ref.[71] , variational ground state wave functions of the Jastrow type incorporating state-dependent correlations (central and tensor) in ref.[72] . Two main features emerge from these calculations : 1) κ is sensitive to the behaviour of the potential at intermediate range (1 to 2 fm), 2) the contribution

of tensor correlations is large (it roughly doubles the value of κ [72]). Results obtained for ^{16}O and ^{40}Ca show some tendency to give a larger value than the experimental one, as expected. The data for heavy nuclei (independence on A) suggest that a relevant comparison can be made between a nuclear matter evaluation of κ and the experimental value for heavy nuclei (with the uncertainties stated at the beginning of this section). Comparison of the computed values with the HJ potential shows that κ is sensitive to the many-body approach as well as the approximations used. The results obtained in ref.[72]suggest that the HJ is more successful than the RSC potential in reproducing the experimental values. The nuclear matter value of ref.[69] should be considered as a rough estimation and an accurate calculation using the Brueckner-Bethe approach is needed.

From the above discussion the following conclusions can be drawn : The TRK evaluation of κ is an interesting test for nuclear matter theories and brings them closer to experiment. The sensitivity to medium range correlations, where the nucleon-nucleon interactions best founded theoretically to date are especially reliable, opens the door towards more fundamental approaches. Let us mention some work already done in this direction [76, 77]. A computation of κ with, for instance, the Paris potential [78], would be desirable. Very accurate measurements for A =2,3 and 4 nuclei, for which calculations are almost exact, would be extremely helpful to push further the comparison between theory and experiment.

5. Some conclusions.

To end up, let us make some general observations :

- the dipole strength is now well known up to around 140 Mev. However, very accurate measurements for the few-body systems are needed. Although our analysis strongly suggests that data from photoabsorption of light nuclei and photoneutron emission of heavy nuclei are consistent (discussion of σ_{-1} and σ_{-2}), a direct experimental check would be desirable.

- the dipole enhancement factor κ should be used as a systematic tool to test nucleon-nucleon potentials and different many-body theories (Bethe-Brueckner and variational). The sensitivity of κ to medium range correlations makes it especiallly suited to test theoretically founded nucleon-nucleon potentials.

- from the experimental values of σ_{-1} one obtains, model independently, very large values for the zero-point Goldhaber-Teller motion of light nuclei. It is suggested that the study of the deexcitation of the giant dipole resonance of light nuclei may provide information on neutron-neutron correlations and/or, eventually, may be used to search multineutron bound states.

- the HF-RPA theory is a reasonable general scheme to study the strength distribution of collective modes. Complete calculations of S(E) and moment evaluations of the strength (sum-rules) are complementary, the later being in some cases especially adequate because they give better physical insight.

- the experimental knowledge of σ_{-1} provides a direct measure of ground state two-body correlations. Selfconsistent RPA calculations are successful in reproducing them.
- the present situation concerning isoscalar quadrupole and monopole strength is experimentally, despite recent major progress, at a much more primitive stage than for the dipole strength. Effort to critically review the analysis of hadron inelastic scattering is needed, in particular to give reliable estimations of the percentage of the EWSR exhausted by the giant resonance.
- the knowledge of dipole, monopole and quadrupole strength puts severe constraints on the parameters of effective forces.
- our analysis indicates that from the present knowledge of isoscalar quadrupole strength a value of the nuclear matter effective mass $m^*/m \simeq 0.75$-0.85 can be inferred.
- similarly, from the present knowledge of isoscalar monopole strength a value of the nuclear matter compression modulus $K_{nm} \simeq 200$-240 Mev can be inferred. This value is consistent with that obtained in the liquid droplet model, by studying nuclear binding energies.
- in addition to the traditional quantities (Fermi momentum $k_F \simeq 1.36$ fm^{-1} and binding energy per particle $E/A \simeq 15$ Mev), we feel that nuclear matter theorists should add $m^*/m \simeq 0.8$, $K_{nm} \simeq 200$-240 Mev and $\kappa \simeq 0.8$-1.0 as relevant parameters that a many-body theory should reproduce.

Acknowlegments

The author is indebted to R. Bergère, J.W. Clark, N.V. Giai, N. Marty, D.G. Sandler and D. Vautherin for discussions and for communicating results prior to publication. Special thanks are due to Bill Dalton for the stimulating atmosphere he succeded to create during the conferende.

References

[1] J.S. Levinger, "Nuclear Photodesintegration", Oxford University Press, Oxford 1960.

[2] "Electro-and Photonuclear Reactions", ed. by S. Costa and C. Schaerf, Lecture Notes in Physics, Vol. 61 and 62, Springer-Verlag 1977

[3] "Nuclear Physics with Electromagnetic Interactions", ed. by H. Arenhövel and D. Drechsel, Springer-Verlag 1979

[4] S. Fallieros, "Electromagnetic interactions and nuclear excitations", Lecture Notes Orsay, 1975.

[5] A. Bohr and B.R. Mottelson, "Nuclear Structure", Vol. II, Benjamin 1975.

[6] G.E. Brown, in ref.[3]

[7] J. Speth, in ref.[3]

[8] D. Drechsel, in ref.[2

[9] H. Arenhövel, in ref.[3]

[10] R. Rosenfelder, Phys. Lett. 79B (1978) 15 ; preprint Mz-TH 79/13

[11] O. Bohigas, A.M. Lane and J. Martorell, Phys. Rep 51 (1979) 267

[12] J.V. Noble, Ann. Phys. 67 (1971) 98

[13] S. Fallieros, in Research Report, Tohoku University Vol. 5, 1972

[14] T.J. Deal and S. Fallieros, Phys. Lett. 44B (1973) 224 ; Phys. Rev. C7 (1973) 1709 ;
E.I. Kao and S. Fallieros, Phys. Rev. Lett. 25 (1970) 827

[15] E. Lipparini, G. Orlandini and R. Leonardi , Phys. Rev.C16 (1977) 812

[16] L.J. Tassie, Autralian Jour. Phys. 9(1956) 407 ; 11(1958) 481 ; Nuov. Cim. 18(1960) 525

[17] B.L. Berman and S.C. Fultz, Rev. of Mod. Phys. 47 (1975) 713

[18] R. Bergère in ref.[2]

[19] J. Ahrens, H. Gimm, A. Zieger and B. Ziegler, Nuov. Cim. 32(1976) 364

[20] J. Ahrens, H. Borchert, K.H. Czock, H.B. Eppler, H. Gimm, H. Gundrum, M. Kröning, P. Riehn, G. Sita Ram, A. Zieger and B. Ziegler, Nucl. Phys. A251(1975) 479

[21] A. Lepr ce, H. Beil, R. Bergère, P. Carlos, J. Fagot and A. Ver ère, Phys. Lett. 79B (1978) 43

[22] R. Bergère in ref.[3] and private communication

[23] W.T. Weng, T.T.S. Kuo and G.E. Brown, Phys. Lett.46B (1973) 329

[24] F.E. Bertrand, Ann. Rev. Nucl. Sci. 26(1976) 457

[25] N. Marty, M. Morlet, A. Willis, V. Comparat, R. Frascaria and J. Kallne, Orsay report IPNO/PhN 75-11, 1975 and Proceedings of the Intern. Symp. on "Highly Excited States in Nuclei", Jülich, Vol.I, p.17, 1975

N. Marty, A. Willis, M. Morlet, R. Frascaria, V. Comparat and P. Kitching, contribution to Symposium on "Large Amplitude Collective Nuclear Motions", Lake Balaton (IPNO-PhN 79-18)

[26] D.H. Youngblood, C.M. Rozsa, D.R. Brown and J.D. Bronson, Phys. Rev. Lett. 39(1977) 1188 and private communication

[27] M. Buenerd, C. Bonhome, D. Lebrun, P. Martin, J. Chauvin, G. Duhamel, G. Perrin and P. de Saintignon, Phys. Lett. 84B (1979) 305

[28] F.E. Bertrand, G.R. Satchler, D.J. Horen and A. van der Woude, Phys. Lett. 80B (1979)198

[29] D.J. Thouless, Nucl. Phys. 22(1961) 78

[30] G.E. Brown, Facets in Physics, Academic Press, N.Y. 1970, p.141

[31] E.R. Marshalek and J. da Providencia, Phys. Rev. C7(1973) 2281

[32] D.M. Brink and R. Leonardi, Nucl. Phys. A258(1976) 285

[33] J. Martorell, O. Bohigas, S. Fallieros and A.M. Lane, Phys. Lett. 60B(1976) 313

[34] O. Bohigas, J. Martorell and A.M. Lane, Phys. Lett. 64B (1976) 1

[35] K. Goeke, A.M. Lane and J. Martorell, Nucl. Phys. A296 (1978) 109

[36] S. Stringari, E. Lipparini, G. Orlandini, M. Traini and R. Leonardi, Nucl.Phys. A309(1978) 177

[37] S. Stringari, E. Lipparini, G. Orlandini, M. Triani and R. Leornardi, Nucl. Phys. A309(1978) 189

[38] M. Kohno and K. Andō, Progr. Theor. Phys. 61(1979) 1065

[39] K.F. Liu and N.V. Giai, Phys. Lett. 65B(1976) 23

[40] N.V. Giai, private communication

[41] D. Vautherin and D.M. Brink, Phys. Rev C5(1972) 626

[42] M. Beiner, H. Flocard, N.V. Giai and P. Quentin, Nucl. Phys. A238(1975) 29

[43] S.A. Moszkowski, Phys. Rev. C2(1970) 402 ;
J.V. Ehlers and S.A. Moszkowski, Phys. Rev. C6(1972) 217

[44] H.S. Köhler, Nucl. Phys. A258(1976) 301

[45] J. Treiner and H. Krivine, J. Phys. G2(1976) 285

[46] H. Krivine, J. Treiner and O. Bohigas, Nucl. Phys. A336 (1980) 155

[47] W. D. Myers, W.J. Swiatecki, T. Kodama, L.J. El-Jaick and E.R. Hilf, Phys. Rev. C15(1976) 2032

[48] B. Ziegler in "Few Body Systems and Electromagnetic Interactions", ed. by C. Ciofi degli Atti and E. De Sanctis, Lecture Notes in Physics, Vol. 86, Springer Verlag 1978

[49] D.M. Brink, Nucl. Phys. 4(1957) 215

[50] A. Dellafiore and D.M. Brink, Nucl. Phys. A286(1977) 474

[51] G.E. Brown and M. Bolsterli, Phys. Rev. Lett. 3(1959) 472

[52] G.E. Brown, J.A. Evans and D.J. Thouless, Nucl. Phys. 24 (1961) 1

[53] V. Bernard, Thèse 3ème cycle, Orsay 1978

[54] N.V. Giai, contribution to the Varenna Summer School, July 1979

[55] E. Lipparini, G. Orlandini, S. Stringari and M. Traini, Nuov. Cim. 42A(1977) 296

[56] O. Bohigas, N.V. Giai and D. Vautherin, to be published

[57] C.W. de Joger, H. de Vries and C. de Vries, Atomic Data and Nucl. Data Tables 14(1974) 479

[58] A.M. Lane and A.Z. Mekjian, Phys. Rev. C8(1973) 1981

[59] A. Migdal, J. Phys. USSR 8(1944) 331

[60] W.D. Myers and W.J. Swiatecki, Ann. Phys. 55(1969) 395 ; 84(1974) 186 ; W.D. Myers, "Droplet Model of Atomic Nuclei", Plenum, New York 1977

[61] J.P. Blaizot, to be published in Phys. Rep.

[62] J.P. Blaizot, D. Gogny and B. Grammaticos, Nucl. Phys. A265 (1976) 315

[63] W. Weise, in ref.[2]

[64] D. Drechsel and Y.E. Kim, Phys. Rev. Lett. 40(1978) 531

[65] W.T. Weng, T.T.S. Kuo and K.F. Ratcliff, Phys. Lett. 52B (1974) 5

[66] M.L. Rustgi, O.P. Rustgi and T.S. Sandhu, Can. J. Phys. 55 (1977) 158

[67] H. Arenhövel and W. Fabian, Nucl. Phys. A292(1977) 429

[68] G. Boutin, B. Goulard and J. Torre, Can. J. Phys. 56 (1978) 1447

[69] A. Arima, G.E. Brown, H. Hyuga and M. Ichimura, Nucl. Phys. A205(1973) 27

[70] W.T. Weng, T.T.S. Kuo and G.E. Brown, Phys. Lett. 46B (1973) 329

[71] M. Gari, H. Hebach, B. Sommer and J.G. Zabolitzky, Phys. Rev. Lett. 41(1978) 288

[72] D.G. Sandler and J.W. Clark, contribution to this conference and preprint

[73] J.G. Lucas and M.L. Rustgi, Nucl. Phys. A112(1968) 503

[74] V.N. Fetisov, A.N. Gorbunov and A.T. Varfolomeev, Nucl. Phys. 71(1965) 305

[75] W.E. Meyerhof and S. Fiarman, Proceedings of Asilomar Conference 1973, ed. by B. L. Berman, Lawrence Livermore Laboratory 1973

[76] J.V. Noble, Nucl. Phys. A290 (1977) 349

[77] G.E. Brown and M. Rho, Stony Brook preprint 1979

[78] R. Vinh Mau, "The Paris nucleon- nucleon potential" in "Mesons and Nuclei", Vol. I, ed. by M. Rho and D. Wilkinson, North Holland 1979

Table Captions

Table 1 Many-body character of operators whose ground-state expectation value gives the low positive moments. Q is assumed to be 1-body and the hamiltonian is H = T(1-body) + V(2-body).

Table 2 Experimental values of σ_{-1} and σ_{-2}: (a) from ref.[17]; (b) from ref.[18]; (c) from refs.[19-20].

Table 3 First column : experimental values of σ_{-1} (see table 2). Third column : experimental charge root mean square radii from ref.[57]. See text for further explanation.

Table 4 Comparison of experimental values of σ_{-1} and σ_{-2} (see table 2) with selfconsistent RPA calculations using different forces. Last column : lower bounds of σ_{-2}. Last two lines : results obtained with eq.(4.21) using the corresponding value of nuclear matter symmetry energy coefficient a_τ.

Table 5 Values of the dipole enhancement factor κ. The experimental values are extracted from σ_0 by integrating the photoabsorption cross-section up to pion threshold. See text for further explanation.

	Q isovector Q_1 ~ [H, Q] ~ 2-body	Q isoscalar [V, Q] = 0, Q_1 ~ [T, Q] ~ 1-body
m_0	2-body *	2-body
m_1	2-body *	1-body *
m_2	4-body	2-body
m_3	4-body	2-body *

Table 1

	$\sigma_{-1} A^{-4/3}$ (mb)		$\sigma_{-2} A^{-5/3}$ ($\mu b . Mev^{-1}$)	
	I	II	I	II
^{7}Li	0.42[c]	0.09[a]	10.6[c]	2.8[a]
^{12}C	0.32[c]	0.067[a]	5.0[c]	1.2[a]
^{16}O	0.36[c]	0.044[a]	5.8[c]	0.74[a]
^{40}Ca	0.33[c]		4.8[c]	
^{90}Zr		0.175[b]		2.3[b]
Sn		0.20 [b]		2.7 ± 0.2[b]
Ce		0.19 [b]		2.5 ± 0.2[b]
Sm		0.21 [b]		2.8 ± 0.2[b]
^{197}Au		0.21 [b]		2.6 ± 0.2[b]
^{208}Pb		0.19 [b]		2.6 ± 0.2[b]

Table 2

	σ_{-1} (exp.) (mb)	$\langle o \vert r^2_{zn} \vert o \rangle^{1/2}$ (fm)	$\langle r^2_c \rangle^{1/2}$ (exp.) (fm)	R	$\overline{R}$	R_{GDR}
^{7}Li	4.64 [c]	1.28	2.41	0.53	0.51	0.68
^{9}Be	5.19 [c]	1.05	2.51	0.42	0.43	0.54
^{12}C	8.81 [c]	1.01	2.45	0.41	0.36	0.53
^{16}O	14.50 [c]	0.97	2.72	0.36	0.29	0.46
^{40}Ca	45.5 [c]	0.69	3.48	0.20	0.16	0.26
^{90}Zr	70.6 [b]	0.39	4.28	0.09	0.09	0.12
^{208}Pb	229.2 [b]	0.31	5.50	0.06	0.05	0.07

Table 3

	$\sigma_{-1} A^{-1/3}$ (mb)		$\sigma_{-2} A^{-5/3}$ (μb.Mev^{-1})					
	Exp.	Theory (ref. [56]) SIII [42]	Exp.	Theory				
				Ref. [56] SIII [42]	Ref. [56] SkM [46]	Ref. [56] Ska [44]	Ref. [56] SII [42]	Refs. [32, 55] SII [42]
^{16}O	0.36[c] 0.044[a]	0.33	5.8[c] 0.74[a]	5.0	5.6	7.7	5.0	4.8
^{40}Ca	0.33[c]		4.8[c]	3.9	4.3	5.8	3.8	3.4
^{90}Zr	0.18[b]		2.3[b]	2.8	2.9	4.0	2.7	2.6
^{208}Pb	0.19[b]	0.22	2.6 ± 0.2[b]	2.6	2.8	3.6	2.5	2.1
				1.9	1.7	1.6	1.6	+ σ_2 (Migdal)
				28.1	31.0	32.9	34.1	+ a_τ (Mev)

Table 4

Table 5

		^{2}H	^{3}He	^{4}He	^{16}O	^{40}Ca	Heavy nuclei	Nuclear matter
THEORY	HJ	0.52 [66]		1.2 [71]	1.4 [71]	1.17 [69]		1.35 [69] 0.7 - 0.9 [72]
	RSC	0.50 [67]	0.79 [64] 0.76 [68]	1.14 [71] 1.27 [70]	1.3 [71] 1.26 [70]	1.15 [70]		1.1 - 1.4 [72]
Exper.		0.35 ± 0.10 [73]	0.75 ± 0.10 [74]	0.63 [75]	1.12 ± 0.05 [20]	1.15 ± 0.10 [20]	0.75 ± 0.15 [21,22]	

Figure captions

Fig.1 Energy of the GDR as a function of A ; a) $EA^{1/6}$ = const. b) $EA^{1/3}$ = const. (from ref.[18]).

Fig.2 a) Experimental values of the widths Γ (FWHM) of the GDR as obtained at Saclay for $90 \leq A \leq 238$ (from ref.[18]) ;
b) values of the integrated cross-section obtained by extrapolating the measured cross-section in the GDR region with Lorentzian shapes (from ref.[17]).

Fig.3 Photoneutron cross-section of lead measured with monochromatic photons (from refs.[21, 22]).

Fig.4 Values of $1 + \kappa$ as a function of mass number extracted from measured σ_0 up to pion threshold (taken from [22], see refs.[20-22]).

Fig.5 Isoscalar giant quadrupole resonance : a) energy as a function of mass number ; b) width ; c) percentage of EWSR exhausted by the resonance (from ref.[24]).

Fig.6 Isoscalar giant monopole resonance : a) energy variation $EA^{1/3}$ = const. ; b) width ; c) percentage of EWSR exhausted by the resonance (data taken from refs.[25-28]).

Fig.7 Monopole and quadrupole isoscalar strength distributions for ^{16}O and ^{208}Pb given by the RPA calculation of ref.[39,40], with the Skyrme SIII force.

Fig.8 Sketch of proton and neutron distributions for light nuclei : (a) ground state, (b) giant dipole resonance.

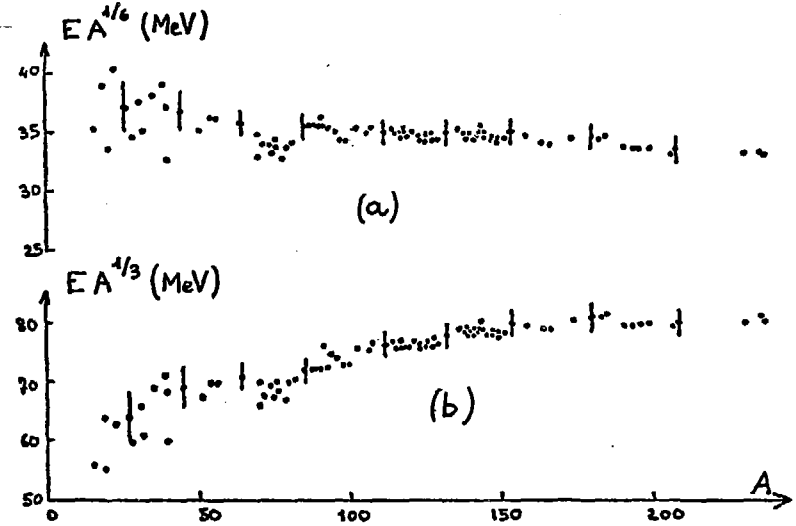

Fig.1

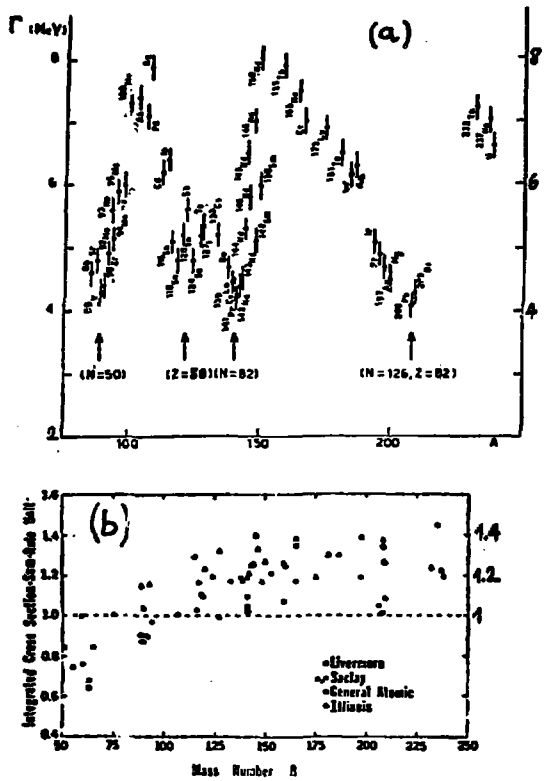
(a)
(N=50)
(Z=50)(N=82)
(N=126, Z=82)
100
150
200
A
(b)
Livermore
Saclay
General Atomic
Illinois
Mass Number A

Fig.2

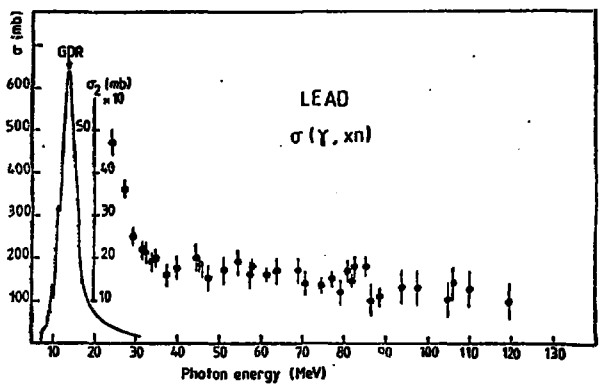
σ (mb)
GDR
σ2 (mb) ×10
LEAD
σ (γ, xn)
600
500
400
300
200
100
50
40
30
20
10
10 20 30 40 50 60 70 80 90 100 110 120 130
Photon energy (MeV)

Fig.3

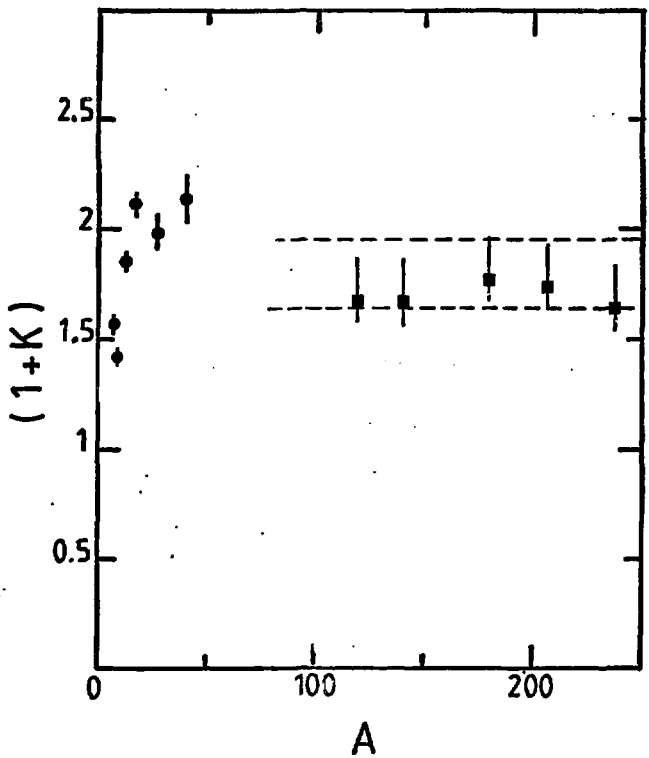

Fig.4

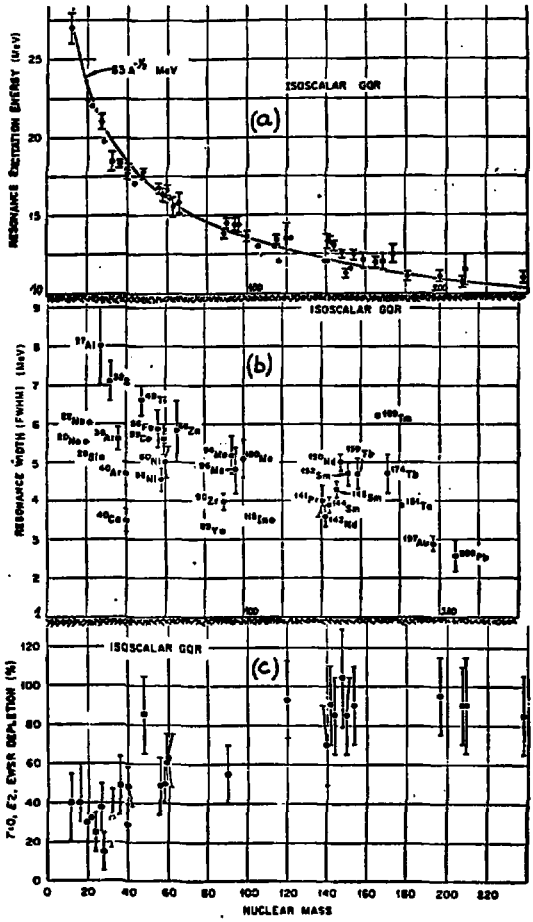
RESONANCE EXCITATION ENERGY (MeV)
63 A^-1/3 MeV
ISOSCALAR GQR
(a)
RESONANCE WIDTH (FWHM) (MeV)
ISOSCALAR GQR
(b)
T=0, E2, EWSR DEPLETION (%)
ISOSCALAR GQR
(c)
NUCLEAR MASS

Fig.5

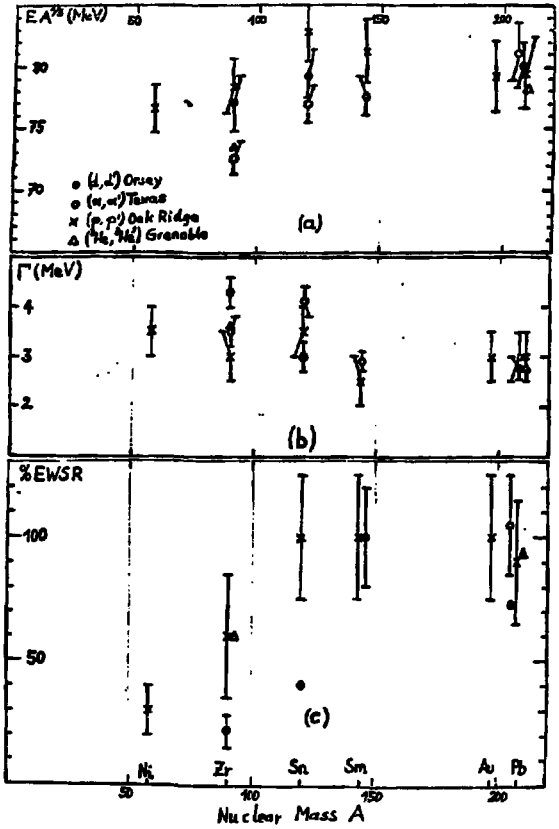
E.A^1/3 (MeV)
80
100
120
140
160
90
75
70
(μ,μ') Orsay
(α,α') Texas
(p,p') Oak Ridge
(3He,3He') Grenoble
(a)
Γ (MeV)
4
3
2
(b)
%EWSR
100
50
(c)
Ni
Zr
Sn
Sm
Au
Pb
50
100
150
200
Nuclear Mass A

Fig.5

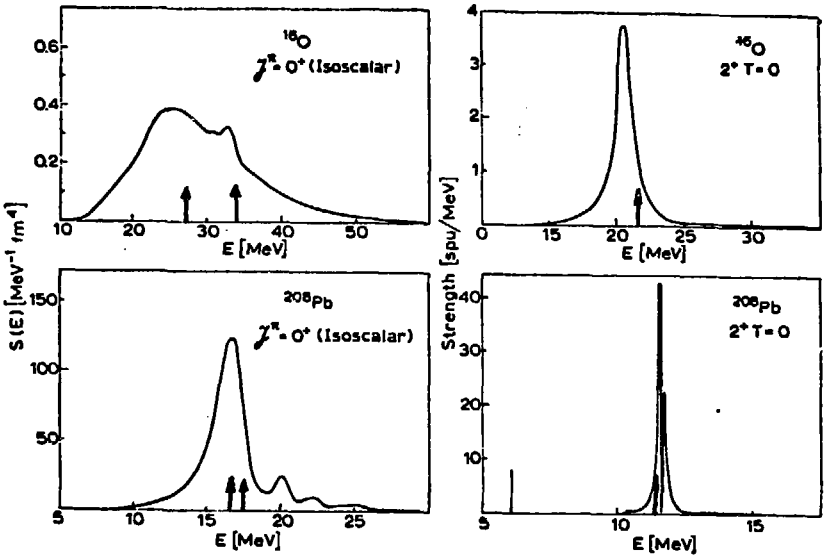
^{16}O
$J^{\pi}=0^{+}$ (Isoscalar)
^{16}O
2^{+} T=0
^{208}Pb
$J^{\pi}=0^{+}$ (Isoscalar)
^{208}Pb
2^{+} T=0
S(E) [MeV^{-1} fm^{-4}]
Strength [spu/MeV]
E [MeV]
E [MeV]
E [MeV]
E [MeV]

Fig.7

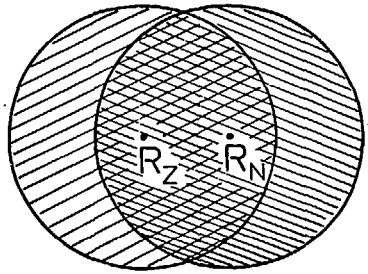

(a)

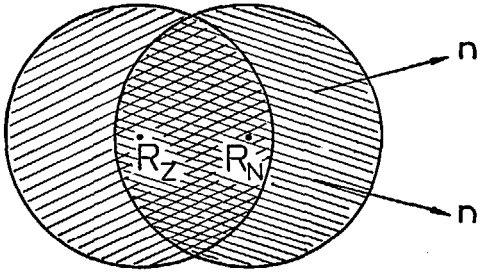

(b)

Fig.8